Influence of porous media on intrusion rate into water distribution pipes

Yan Yang, Tuqiao Zhang and David Z. Zhu

ABSTRACT

Untreated water can intrude into water distribution systems through pipe leaks and cracks when negative pressure events occur inside drinking water pipelines. The orifice equation is typically used for calculation of intrusion flow rate, which ignores the impact of the soil surrounding the pipeline. This paper presents the results of an experimental study on the effect of porous media surrounding pipelines and the flow Reynolds number on intrusion flow rate for a circular orifice. The porous media, orifice size, and flow regime affect the discharge coefficient of the orifice equation. A new expression was suggested for predicting the intrusion flow rate. A discontinuity in the discharge coefficient was also found at a large Reynolds number. The effect of the pipe curvature on the discharge coefficient was found to be insignificant.

Key words | contaminant intrusion, discharge coefficient, orifice equation, porous media, water distribution system

Yan Yang
College of Civil Engineering and Architecture,
Zhejiang University,
A810 Anzhong Building, Hangzhou 310058,
China

Tuqiao Zhang
College of Civil Engineering and Architecture,
Zhejiang University,
A511 Anzhong Building, Hangzhou, 310058,
China

David Z. Zhu (corresponding author)
College of Civil Engineering and Architecture,
Zhejiang University,
Hangzhou, 310058,
China
and
Department of Civil and Environmental
  Engineering,
University of Alberta,
Edmonton, AB, Canada T6G 2W2
E-mail: david.zhu@ualberta.ca

NOMENCLATURE

a constants in Equation (2)

A cross-section area of orifice

C fitted parameter in Equation (3)

C_d discharge coefficient

d orifice diameter

g gravitational acceleration

ΔH difference between the external and internal pressure head

i hydraulic gradient in porous media

m non-Darcy exponential

Q intrusion flow rate

Re   Reynolds number

v macroscopic velocity in porous media

V average flow velocity at the orifice

ν kinematic viscosity of water

INTRODUCTION

Low or negative pressure events may occur in drinking water distribution systems (Gullick et al. 2005), which can cause surrounding groundwater being intruded into the distribution systems through various types of pipe cracks and defects (Karim et al. 2003). Water pipes are usually located below the ground with a certain thickness of soil cover above the pipeline. Contaminated soil and groundwater surrounding the pipes may contain mixtures of microbial or chemical contaminants (Karim et al. 2003; He et al. 2009; Besner et al. 2010; Payne et al. 2010). Even if leaking pipes are located above the ground water table, the leak will provide a constant feed of water into the surrounding soil, while the contaminated water can intrude into the pipeline during negative pressure events. Intrusion of contaminants from the soil-groundwater environment surrounding the pipe into water distribution system has been widely recognized as a significant health threat (Karim et al. 2003; Besner et al. 2011).

Intrusion is usually seen as a reverse leakage. Pipe leaks can occur over various kinds of defects (e.g. orifices, longitudinal cracks, circumferential cracks) (Greyvenstein & van Zyl 2007; Guo et al. 2013). In order to compute intrusion

volumes, commercial surge models typically simplify the pipe defects to circular orifices, and the diameter of these orifices is computed based on the leakage rate of the system (Kirmeyer *et al.* 2001; Ebacher *et al.* 2012). So the understanding of flow through circular orifices is important. The orifice equation is commonly used for the calculation of the intrusion flow rate (Besner *et al.* 2011; Mora-Rodriguez *et al.* 2012):

$$Q = C_d A \sqrt{2g\Delta H} \tag{1}$$

where Q is the intrusion flow rate, C_d is the discharge coefficient, A is the cross-section area of the orifice, g is the gravitational acceleration, ΔH is the difference between the external pressure head and internal pressure head. Many factors affect the discharge coefficient, such as the ratio of the orifice diameter to the pipe wall thickness, the sharpness of the edge of the orifice, the roughness of the inner surface, the type of orifice plate (plane or curved), and water viscosity (Brater & King 1996).

The orifice equation is commonly used to compute intrusion flow rate without the consideration for the surrounding soil. Many researchers investigated the role of soil hydraulics on the pressure-leakage (under positive pressure conditions in pipes) relationship. A simplistic application of Darcy's law suggests the flow rate should be linearly proportional to the pressure head in the pipe. Considering the interactions of the external soil properties, the water flow and the pipe leaks are complex, the relationship between pressure and flow rate is unlikely to be linear (Van Zyl & Clayton 2007). Walski *et al.* (2006) compared the head loss caused by orifice losses and porous media losses when modeling the flow from leaks. They pointed out that orifice head loss dominates in most water distribution systems, and the orifice equation is suitable for modeling leaks for a fixed-size circular hole. Coetzer *et al.* (2006) conducted an experimental study to determine the effect of the media surrounding the pipe leakage on its hydraulic behavior, and found that the flow rate for a given pressure could be higher when the media surrounding the leak is under some special conditions. This result is somewhat counterintuitive, indicating the interesting interaction of porous media and the orifice. Collins *et al.* (2010) and

Collins & Boxall (2013) presents a new analytical expression to describe the contaminants intrusion which considers the viscous and inertial resistance of porous media, and compares with the results of computational fluid dynamics (CFD) models and experiments. The new expression indicates a linear relationship between the flow rate and pressure difference when the pressure difference is small or the viscous resistance of the soil significantly exceeds the inertial resistance. It also reduces to the orifice equation when no resistance presents in the external porous media. It is shown that the existence of a surrounding porous media decreases the intrusion flow rate from that predicted by the standard orifice equation. The analytical expression tends to under-estimate the intrusion rate compared with the experimental results. Mansour-Rezaei & Naser (2012) used a combination of dimensional analysis and a two-dimensional finite element model to find the relationship among the effective factors. The results show that the exponent of pressure difference was about 2/3, and the effect of orifice area was lower than that in the orifice equation.

The present study has three objectives. The effect of surface type on intrusion flow rate is studied in Experiment (Exp.) 1. Pipe defects are generally located in a curved surface, while orifices are generally located in plane surface in the traditional theory. Exp. 2 studies the effect of porous media surrounding pipelines, as the characteristics of porous media affects the intrusion flow. The effect of flow at a large Reynolds number is studied in Exp. 3, as the intrusion flow is unlikely to be laminar.

METHODS

Experimental apparatus

This study investigated the flow discharged through porous media into an orifice on the pipe wall. The low or negative pressure inside the pipe is not directly modeled. Instead, the atmosphere pressure was used inside the pipe in this study. This difference is not believed to be important as the intrusion flow is driven by the relative pressure head difference between the inside and outside of the pipe. Figure 1(a) shows the schematics of the experimental
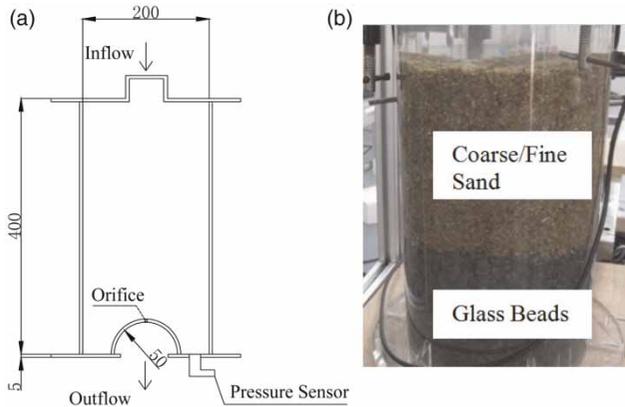
Figure 1 | (a) Schematics of the experimental setup (all dimensions are in millimeters); (b) experimental setup with porous media in Exp. 2.

setup. It consisted of a plexiglass cylindrical container filled with porous media and had an orifice at the center of the bottom. The container was connected to a water tank which supplied the water with required pressure head. A pressure sensor (Model XSE/A-H1|T2B1V0N; Westzh Technologies) with an accuracy of 0.05 kPa was used to measure the pressure at the entrance of the orifice. A camera was used to record the experimental process. The outflow was discharged freely through the orifice. All the experiments were carried out at a room temperature of 23 °C.

The height of the container was 400 mm, the inner diameter was 200 mm, and the thickness of the container bottom was 5 mm. The top of the container could be opened for sand loading. A curved bottom and a plane bottom were used in the experiments. Half round pipe was used to form a curved surface (Figure 1(a)), which had a diameter of 100 mm and a length of 140 mm. Two orifice sizes were used: 2.2 and 4.2 mm. The orifices were sharp-edged. The pressure sensor was installed on the bottom of the container. The difference in the elevations of the pressure sensor and the orifice entrance was subtracted from the pressure sensor readings. Atmospheric pressure corresponds to a gauge pressure value of 0, thus the reading of pressure sensor is equal to the difference between external pressure and internal pressure of the orifice.

Permeability of the porous media

Flow rate through a porous media depends on permeability and pressure gradient. The Darcy equation assumes a linear relation between the pressure gradient and the flow rate, which is suitable for low Reynolds number. Under high pressure gradients, there is a nonlinear relationship between the flow rate and the pressure gradient in most surrounding soil during intrusion, thus the Darcy's law is not valid. Different laws have been proposed like Forchheimer's or Izbash's law (Bordiera & Zimmer 2000). This study employs the Izbash equation (Izbash 1931) to simulate flow in porous media as it is an extension of the Darcy's law:

$$i = -av^m \tag{2}$$

where i is the hydraulic gradient; v is the macroscopic velocity, a and m are constants related to the properties of the porous media and the fluid, m is non-Darcy exponential. The equation becomes Darcy's law when $m = 1$, and the flow is fully turbulent when $m = 2$ (Venkataraman & Rao 1998).

Three kinds of surrounding media were used in the experiments: homogeneous glass beads, homogeneous coarse sand and well-graded fine sand. The particle size of homogeneous glass beads is from 4 to 6 mm, with an average size of 5 mm. The particle size of homogeneous coarse sand is from 1.18 to 2.36 mm, with an average of 1.77 mm. Figure 2 shows the cumulative grain size distribution of the fine sand. The permeability of the three kinds of porous media is tested using a similar apparatus as that of Zhang *et al.* (2013). The non-Darcy exponential of three kinds of porous media m is respectively 2 for glass beads, 1.31 for the coarse sand, and 1.04 for the fine sand.

Experimental procedures

Preparatory work included adjusting the container bottom to be horizontal and packing porous media in the container. The orifice was first plugged with a rubber stopper. In order to ensure no relative movement of particles, the maximum hydraulic pressure in the experiments was applied to the porous body for more than 12 hours to make the particles compacted. Experiments were started by unplugging the rubber stopper, and adjusting the water level in the water tank to the desired value. After several minutes of waiting to ensure that the head was steady-state, the flow rate was measured by the time/weight method by collecting the
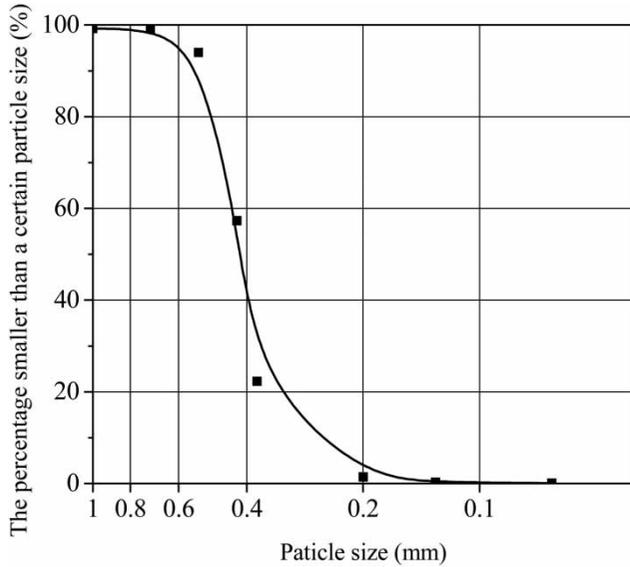
Figure 2 │ Cumulative grain size distribution of fine sand.

outflow through the orifice over a period of time. This process and the related pressure sensor readings were recorded in the same video images. The videos recorded at 40 frames per second, so the time could be accurate to 0.025 seconds. The weight of the water was measured by an electronic balance (with an accuracy of 0.1 g). The pressure readings were also averaged. The pressure was increased in a stepwise fashion then decreased after reaching the maximum value in the experiments.

Table 1 shows the details of the experimental conditions in this study. Exp. 1 has no porous media in the container to exclude the influence of porous media. The porous media in Exp. 2 consisted of two layers as shown in Figure 1(b). The lower layer was glass beads, and the top layer was coarse

Table 1 │ List of experiments

	Porous media	Surface type	Orifice size (mm)
Exp. 1	No media	Curved	2.2
			4.2
		Plane	2.2
			4.2
Exp. 2	Glass beads and coarse sand	Curved	2.2
			4.2
	Glass beads and fine sand		2.2
			4.2
Exp. 3	Glass beads	Curved	4.2

sand or fine sand. The thickness of the glass beads layer was 85 mm and the thickness of coarse/fine sand layer was 170 mm. This arrangement could prevent small sand particles leaking into the orifice. The smooth glass beads were used as porous media in Exp. 3 for its large permeability.

In China, sand is generally used as backfill material around pipes. The coarse and fine sand used in our experiments have similar properties as the sand used in China. Thus this research did not consider the effect of the soil/clay around pipes. The physical characteristics of the porous media related to the intrusion flow is the permeability of the sand layers, not the glass beads. We have carried out experiments to test the effect of glass beads, and the results indicated that the presence of glass beads has no effect on porous media permeability.

RESULTS AND DISCUSSION

Effect of surface type

Figure 3 shows the $\Delta H - Q$ curves with different diameters and surface types for Exp. 1 without media. The curves are fitted with Equation (1), and it can be seen that the square root relationship is suitable for both the orifice on the curved and plane surfaces. The discharge coefficient C_d are 0.69 and 0.71 – for the 2.2 mm orifice on curved and
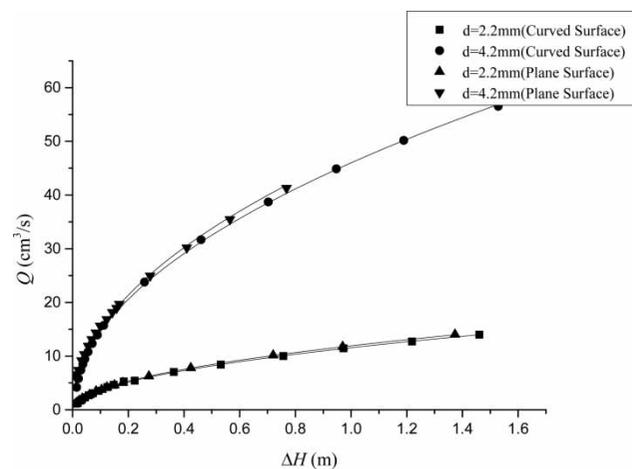

Figure 3 │ $\Delta H - Q$ curves for different orifice diameters and surface types in Exp. 1 without media.

plane surface. An orifice with a length (pipe thickness) to diameter ratio between 2 and 3 is called a tube, so the 2.2 mm orifice is a tube. According to Brater & King (1996), values of discharge coefficient for short tubes were found to vary from approximately 0.72 to 0.83. The values of C_d provided confidence that experiments results are consistent with these. C_d is 0.75 and 0.78 for the 4.2 mm orifice on curved and plane surface, respectively. They are a little larger than a typical value for an orifice, which is around 0.6. This is probably because the 4.2 mm orifice is slightly convergent, which could increase the discharge coefficient.

The orifice discharge coefficient on curved surface is slightly different from that on plane surface. Brater & King (1996) pointed out that if the plate were slightly warped inward, the coefficient of contraction would decrease. It can be seen that C_d on inward-projecting cylindrical surface is slightly smaller than that on the plane surface in our experiments, but the difference is small.

Effect of porous media

Figure 4(a) shows the $\Delta H - Q$ curves for different orifice sizes and porous media, and Figure 4(b) shows the dependence of discharge coefficient on the Reynolds number at the orifice. The discharge coefficient C_d is calculated using Equation (1). The Reynolds number is defined by: $\mathrm{Re} = Vd/\nu$, where V is the average flow velocity at the orifice, d is the orifice size, and ν is the kinematic viscosity of water. The range of Reynolds number is 350 to 10,000.

It can be seen from Figure 4(a) that the presence of porous media changed the flow rate compared with the no media situation, and it has a more pronounced effect for larger diameter orifices. In Figure 4(b), C_d is no longer a constant as in a standard orifice case. Each curve could be divided into three regimes when $\mathrm{Re} < 2000$, between 2000 and 4000, and $\mathrm{Re} > 4000$. These values are believed to be related to the interaction of the porous media seepage and the orifice flow. C_d increases with Re when $\mathrm{Re} < 2000$. When $\mathrm{Re} > 4000$, C_d becomes constant and is independent of Re. For the 4.2 mm orifice, the presence of porous media decreases the flow rate significantly, and C_d with coarse sand media is larger than that with fine sand media, but the difference is small. For the 2.2 mm orifice, the presence of porous media had
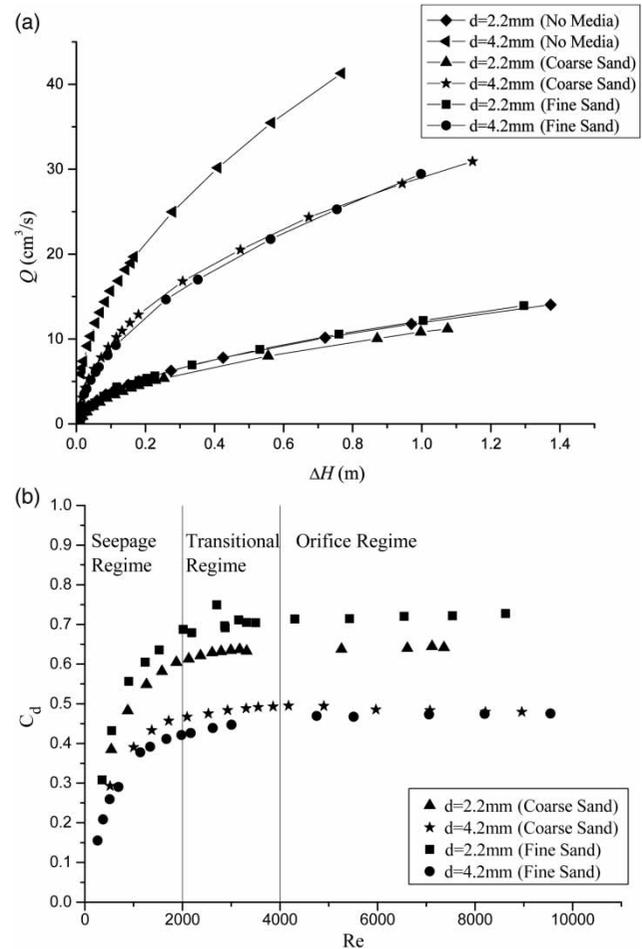

Figure 4 │ Intrusion flow rate with different orifice diameters and porous media: (a) ΔH-Q curves; (b) C_d-Re curves.

smaller impact on the flow rate. C_d with fine sand media is larger than that with coarse sand media. It seems counterintuitive. Particles, especially those located near the orifice, likely obstruct part of the orifice and modify intrusion jet behavior. The porous media has a resistance on the flow into the orifice and also could inhibit the contraction of the flow into the orifice. This phenomenon fully illustrates that the coupled porous media and orifice is a complex system, and the traditional orifice equation is not enough to describe the flow.

Liu *et al.* (2001) demonstrated that there are similarities between flow through porous media and flow through orifices. The pressure drop for flow through the coupled porous media and orifice can be described by developing flow in short ducts and has similar predictable pressure

drop expression as that for flow through porous media. The orifice becomes an extension of the fluid path through the pores. It can be seen from Equation (2) that the pressure drop is proportional to the *m*th power of flow rate in porous media. A relationship similar to the Izbash equation can be used to relate the pressure difference and flow rate:

$$Q = C\Delta H^{1/m} \tag{3}$$

where C is a fitted parameter, which will be discussed later. When Re < 2000, the pressure drop is caused by the frictional losses through porous media and along the wall of orifices which are mainly viscous force. This regime will be called seepage regime here. The relationship of flow rate and pressure drop is mainly determined by the nature of the media, and the value of m is 1.04 for fine sand and 1.31 for coarse sand in our experiments. When Re > 4000, flow in this regime is fully turbulent, and $m = 2$. It is similar to the orifice equation, and could be named orifice regime. The range of Re from 2000 to 4000 is transitional regime, m value is uncertain in this regime. The $\Delta H{-}Q$ curves are fitted in the seepage regime and the orifice regime, which is segmented according to the range of Re obtained from the $C_d{-}Re$ curves.

It can be seen from Table 2 that the experimental results fit well with Equation (3) in the seepage regime and orifice regime. The coefficient C is related to orifice size, flow regime, permeability of porous media, and the local geometry of the particle around the orifice. The values of C are larger for a large diameter orifice. The influence of media permeability to C is different in different regimes. The values of C are inversely proportional to the media permeability in the seepage regime, and they are approximately equal for different media in the orifice regime.

Effect of the Reynolds number

Experiments were repeated under higher water head to study the effect of much larger Reynolds number. A discontinuity can be seen from the $C_d{-}Re$ curve (Figure 5(a)). The C_d suddenly changes from 0.57 to 0.46 when Re is about 16,000–17,000. The pattern is similar when Re is reduced from large to small. This result is in conformity with the findings reported by Coetzer *et al.* (2006) in their study of the effect of pressure on leakage in distribution systems. They suggested that this discontinuity is possibly due to the separation of the fluid stream from the wall.

The surrounding porous media is composed of curved and meshed passages for flow, and the cross-sectional area of the passages may change. So the flow behavior is different from that without media situation. As Re increases, the bending at the surface of microscopic solid causes the stream line to move gradually. The fluid stream may separate from the passage wall at a certain Reynolds number. For further research on the fluid stream separation, we made an arbitrary orifice by hands on the bottom of the container to simulate the curved passage with changing cross-sectional area, and no media is loaded in the container. The passage had a cross-section of non-axisymmetric, and one side of the inclination angle was about 10°. The surface of the passage was rough, and could be polished with sandpaper. We repeated the above experiments before and after polishing.

Figure 6 shows the flow before and after the fluid stream separation extracted from the experiment video with gradually increasing Re. The jet was much more divergent (Figure 6(a)) until a part of fluid stream gradually deviated from the original direction (Figure 6(b)). Finally, the jet showed a constrictive appearance, and a vena contracta appeared downstream of the orifice (Figure 6(c)). This shape was maintained with further increase of the Reynolds number. Figure 5(b) shows the $C_d{-}Re$ curve of the

Table 2 | The fitting equations of ∆H-Q curves with different porous media

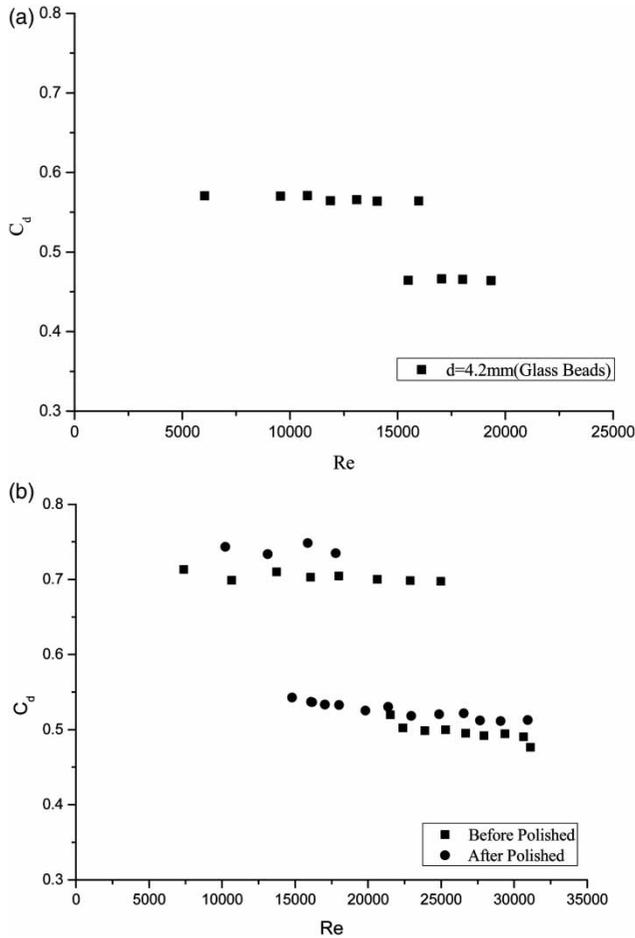| Media	Orifice size (mm)	Seepage regime	R^2	Orifice regime	R^2
Course sand	2.2	$Q = 19.67\Delta H^{1/1.31}$	0.995	$Q = 10.78\Delta H^{1/2}$	0.999
	4.2	$Q = 68.34\Delta H^{1/1.31}$	0.996	$Q = 29.39\Delta H^{1/2}$	0.997
Fine sand	2.2	$Q = 47.39\Delta H^{1/1.04}$	0.966	$Q = 12.15\Delta H^{1/2}$	0.999
	4.2	$Q = 125.39\Delta H^{1/1.04}$	0.984	$Q = 29.13\Delta H^{1/2}$	0.998

Figure 5 │ C_d-Re curves: (a) with glass beads as porous media for a 4.2 mm orifice; (b) before and after polishing for an arbitrary orifice with no porous media.
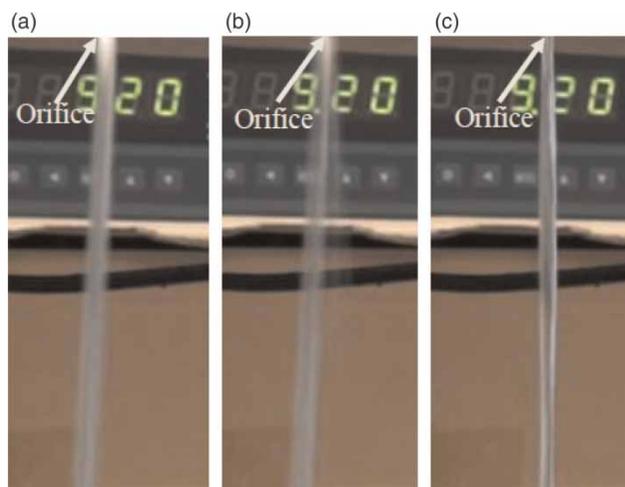

Figure 6 │ Flow forms before and after fluid stream separation for an arbitrary orifice with no porous media (the arrows indicate the location of the orifice).

experiment results before and after polishing. After the fluid stream separation, the discharge coefficient decreased as the flow contracted. As Re decreased with the decrease in the flow rate, C_d still remained the value after the separation. Thus there was a range of Re corresponding to two values of C_d. The surface of the passage became smoother after being polished, the friction head loss reduced. As a result, C_d increased slightly compared to the value before polishing. The Reynolds number corresponding to the discontinuity was smaller after being polished, which indicates that the fluid stream separation is related to the roughness of the passage.

CONCLUSIONS

This study investigated the influence of porous media on the intrusion flow rate through orifices. The intrusion is assumed to occur under steady-state conditions, flow through orifices discharging free liquid jets into air. The porous media in the surrounding environment of the orifice is fully-saturated, homogeneous and isotropic. Experimental results show that the traditional orifice equation is suitable for both the orifice on curved surface and plane surface when there is no porous media surrounding the orifice. The orifice discharge coefficient on the inward curved surface is smaller than that on the plane surface, but the difference is relatively small.

The presence of porous media could change the discharge coefficient and added dependencies on the orifice size, flow regime, and permeability of porous media. A function similar to the Izbash equation is suggested for describing the relationship of the pressure head difference and the flow rate, which fits well with the experimental data both in seepage regime and orifice regime. This expression describes well the complex nature of the flow where the flow is impacted by both the porous media and the orifice. It should be pointed out, however, that further research is needed to develop a general equation for practical use.

There is a discontinuity in the discharge coefficient at large Reynolds number (Re > 10,000) when the porous media is composed of curved and meshed passages for flow. The value of discharge coefficient may change due to

the movement of the stream line, leading to changes in the flow rate. This is different from the continuum hypothesis. Previous research simplified the porous media as a continuous media is inappropriate.

ACKNOWLEDGEMENTS

REFERENCES

Besner, M. C., Broseus, R., Lavoie, J., Di Giovanni, G., Payment, P. & Prevost, M. 2010 Pressure monitoring and characterization of external sources of contamination at the site of the payment drinking water epidemiological studies. *Environ. Sci. Technol.* **44** (1), 269–277.

Besner, M. C., Prévost, M. & Regli, S. 2011 Assessing the public health risk of microbial intrusion events in distribution systems: Conceptual model, available data, and challenges. *Water Res.* **45** (3), 961–979.

Bordiera, C. & Zimmer, D. 2000 Drainage equations and non-Darcian modelling in coarse porous media or geosynthetic materials. *J. Hydrol.* **228** (3–4), 174–187.

Brater, E. F. & King, H. W. 1996 *Handbook of Hydraulics*. McGraw-Hill, New York.

Coetzer, A. J., Van Zyl, J. E. & Clayton, C. R. I. 2006 An experimental investigation into the turbulent-flow hydraulics of small circular holes in plastic pipes. In: *8th Annual Water Distribution Systems Analysis Symposium*. Cincinnati, Ohio, USA, pp. 1–9.

Collins, R. & Boxall, J. 2013 The influence of ground conditions on intrusion flows through apertures in distribution pipes. *J. Hydraul. Eng.* **139**, 1052–1061.

Collins, R., Besner, M. C., Beck, S., Karney, B. & Boxall, J. 2010 *Intrusion Modelling and Effect of Groundwater Conditions*. Water Distribution System Analysis, Tucson Arizona, USA, pp. 585–594.

Ebacher, G., Besner, M. C., Clément, B. & Prévost, M. 2012. Sensitivity analysis of some critical factors affecting simulated intrusion volumes during a low pressure transient event in a full-scale water distribution system. *Water Res.* **46**, 4017–4030.

Greyvenstein, B. & Van Zyl, J. E. 2007 An experimental investigation into the pressure–leakage relationship of some failed water pipes. *J. Water Supply Res. T.* **56** (2), 117–124.

Gullick, R. M., LeChevallier, M. W., Case, J., Wood, D. J., Funk, J. E. & Friedman, M. J. 2005 Application of pressure monitoring and modelling to detect and minimize low pressure events in distribution systems. *J. Water Supply Res. T.* **54** (2), 65–81.

Guo, S., Zhang, T., Zhang, Y. & Zhu, D. Z. 2013 An approximate solution for two-dimensional groundwater infiltration in sewer systems. *Water Sci. Technol.* **67** (2), 347–352.

He, X. Q., Cheng, L., Zhang, D. Y., Li, W., Xie, X. M., Ma, M. & Wang, Z. J. 2009 First molecular detection of group A rotaviruses in drinking water sources in Beijing, China. *Bull. Environ. Contam. Toxicol.* **83**, 120–124.

Izbash, S. 1931 *O Filtracii V Kropnozernstom Materiale*. Leningrad, USSR.

Karim, M. R., Abbaszadegan, M. & Lechevallier, M. 2003 Potential for pathogen intrusion during pressure transients. *J. Am. Water Works Assoc.* **95** (5), 134–146.

Kirmeyer, G. J., Friedman, M., Martel, K., Howie, D., LeChevallier, M., Abbaszadegan, M., Karim, M., Funk, J. & Harbour, J. 2001 *Pathogen Intrusion into the Distribution System*. American Water Works Association Research Foundation, Denver, CO.

Liu, S., Afacan, A. & Masliyah, J. H. 2001 A new pressure drop model for flow-through orifice plates. *Can. J. Chem. Eng.* **79**, 100–106.

Mansour-Rezaei, S. & Naser, G. H. 2012 Contaminant intrusion in water distribution systems: an ingress model. In: World Environmental and Water Resources Congress 2012. Albuquerque, New Mexico, USA, pp. 3002–3010.

Mora-Rodriguez, J., Lopez-Jimenez, P. A. & Ramos, H. M. 2012 Intrusion and leakage in drinking systems induced by pressure variation. *J. Water Supply Res. T.* **61** (7), 387–402.

Payne, S. J., Besner, M. C., Lavoie, J., Krentz, C., Hansen, L. T., Friedman, M., LeChevallier, M. W., Prevost, M. & Gagnon, G. A. 2010 Molecular techniques and data integration: investigating distribution system coliform events. *J. Water Supply Res. T.* **59** (5), 298–311.

Van Zyl, J. E. & Clayton, C. R. I. 2007 The effect of pressure on leakage in water distribution systems. *P. I. Civil Eng.-Water M.* **160** (2), 109–114.

Venkataraman, P. & Rao, P. R. M. 1998 Darcian, transitional, and turbulent flow through porous media. *J. Hydraul. Eng.* **124** (8), 840–846.

Walski, T., Bezts, W., Posluszny, E. T., Weir, M. & Whitman, B. E. 2006 Modeling leakage reduction through pressure control. *J. Am. Water Works Ass.* **94** (4), 147–155.

Zhang, Y., Liu, W., Shao, W. & Yang, Y. 2013 Experimental study on water permittivity of woven polypropylene geotextile under tension. *Geotext. Geomembranes* **37**, 10–15.